Dalton Transactions

PAPER

View Article Online
View Journal | View Issue

Cite this: *Dalton Trans.*, 2014, **43**, 5707

A ferrocene–pyrene based '*turn-on*' chemodosimeter for Cr^{3+} – application in bioimaging†

Mandeep Kaur,[a] Paramjit Kaur,*[a] Vikram Dhuna,[b] Sukhdev Singh[b] and Kamaljit Singh*[a]

Received 17th December 2013,
Accepted 23rd January 2014

DOI: 10.1039/c3dt53536c

www.rsc.org/dalton

Structurally simple, ferrocene–pyrene imine dyad **1** has been developed as a '*turn-on*' chemodosimeter for Cr^{3+}. The sensing event is based upon the hydrolysis of the imine functionality. Further, **1**, which is also non-cytotoxic (100% cell viability), detects intracellular Cr^{3+} in the human breast cancer (MCF-7) cells.

1. Introduction

Chromium, one of the most common elements in the earth's crust and seawater, exists principally as metallic (Cr^0), trivalent (+3), and hexavalent (+6) forms. While the more common trivalent chromium is essential and found in most food and nutrient supplements, the hexavalent chromium is highly toxic. The trivalent chromium has a profound impact on glucose metabolism and is implemented to counter diabetes, cardiovascular and nervous system disorders, *etc.*[1] Exposure to high levels of Cr^{3+} can also have an adverse effect on normal enzymatic activities and cellular structures.[2] Furthermore, the release of excess of Cr^{3+} poses a serious threat to the environment.[3] In the absence of simple methods, development of chemosensors for Cr^{3+}, relying specifically on cost-effectiveness, efficiency and biocompatibility, could provide a viable alternative to the often intricate and expensive methods based on inductively coupled plasma mass spectrometry, atomic absorption, *etc.*[4] Owing to the tendency of the paramagnetic Cr^{3+} to quench fluorescence emission,[5] generally a '*turn-off*' response is observed in sensing events; there are very limited reports[6] wherein a '*turn-on*' response has been reported during sensing of Cr^{3+}. We have in the past reported[7] donor–acceptor dyads for metal ion sensing which showed variable optical responses upon detecting different analytes. Usually, a donor (D) of ferrocene type turns the fluorescence of pyrene '*off*' when used as an acceptor (A) in the D–A dyads through PET or related photophysical processes as discussed later in this paper. Upon interrupting the quenching process, the fluorescence, if '*turn-on*', furnishes an efficient fluorescent probe for different analytes. We previously reported a dyad of ferrocene and 2-(3,5,5-trimethylcyclohex-2-enylidene)malononitrile for the efficient detection of Cu^{2+} which acted through complexation of Cu^{2+} with ferrocene as well as the alkene bridge.[7c] The linker alkene provided an additional coordination site to the metal ion which as a consequence caused electronic perturbation in the D–A receptor leading to the sensing process. However, in the present case, as we describe below in the case of a new D-imine-A dyad, the imine functionality breaks in a metal triggered hydrolysis reaction in the presence of Cr^{3+} and leads to the application of this dyad as an efficient chemodosimeter. Similar chemodosimeters proceeding through hydrolysis reaction have received some attention in the past.[8] However, in such reports, either the detection limit and/or the time required for the completion of the process has not been mentioned, which constitute important parameters of a detection process.[8a,c]

In continuation of our research interest, we report the synthesis and chemodosimeter behaviour of a structurally simple and new dyad (1*E*)-*N*-(ferrocenylmethylene)pyren-1-amine **1** (Scheme 1), which unequivocally depicted an

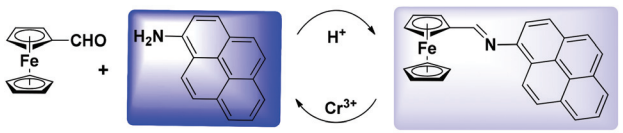

Scheme 1 Synthesis and Cr^{3+} induced hydrolysis of chemodosimeter **1**.

[a]*Department of Chemistry, UGC-Center for Advanced Studies-I, Guru Nanak Dev University, Amritsar-143 005, Punjab, India. E-mail: paramjit19in@yahoo.co.in, kamaljit19in@yahoo.co.in; Fax: +91-183-2258819-20*
[b]*Department of Molecular Biology and Biochemistry, Guru Nanak Dev University, Amritsar-143 005, Punjab, India*

†Electronic supplementary information (ESI) available: Spectral data of **1**, contour surfaces, TD-DFT data, Cartesian co-ordinates and complete ref. 12. See DOI: 10.1039/c3dt53536c

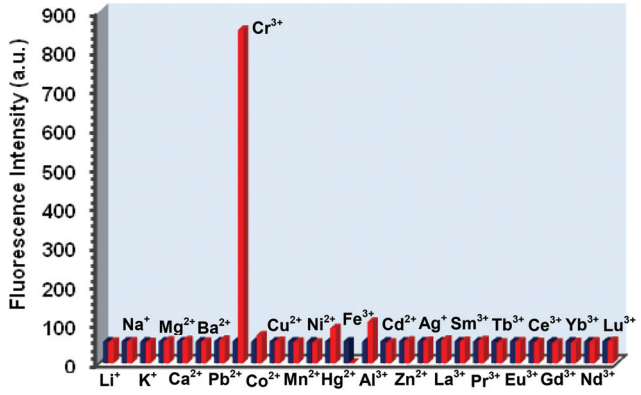

Fig. 1 Changes in the emission properties of **1** (5.0×10^{-6} M, in THF) (blue) at 442 nm upon addition of various metal ions (5.0×10^{-4} M, in water) (red). (The v/v ratio of THF and H_2O in the mixture was 1 : 99.)

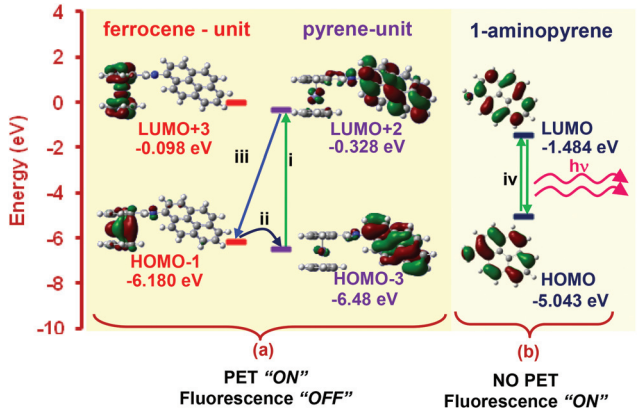

Fig. 2 HOMO–LUMO energy levels of (a) **1** and (b) free 1-aminopyrene.

efficient fluorescence '*turn-on*' chemodosimetric response in the presence of Cr^{3+} in comparison with competitive metal ions (Fig. 1). To the best of our knowledge, **1** constitutes an exclusive example of a simple, ferrocene–imine–pyrene chemodosimeter for the detection of Cr^{3+}. We also furnish robust evidence that the sensing event operates *via* a metal ion promoted hydrolysis of imine functionality of **1**, as the by-products: 1-aminopyrene and 1-ferrocenecarboxaldehyde have been isolated from the sensing experiment as depicted in Scheme 1. The most attractive feature of **1** is the fact that it exhibits rarely observed '*turn-on*' behaviour in the presence of paramagnetic Cr^{3+}.

2. Results and discussion

2.1. Synthesis and characterization

Chemodosimeter **1** was synthesized in one step in 74% yield *via* the simple acid catalysed Schiff-base condensation reaction of 1-ferrocenecarboxaldehyde and 1-aminopyrene (Scheme 1). **1** depicted satisfactory spectroscopic [^{1}H and ^{13}C NMR, ESI-MS, and FT-IR (Fig. S1–S4, see ESI†)] and microanalytical data.

2.2. Behaviour of 1 towards cations

The fluorescence spectrum of **1** (5×10^{-6} M in THF, λ_{exc} = 350 nm) is characterized by a weak emission band peaking at 445 nm attributed to the monomer emission[9] of **1** albeit with low quantum yield (Φ = 0.016), which is characteristic[10] of the quenched emission of pyrene *via* either photoinduced electron transfer (PET) or energy transfer from the ferrocenyl-imine unit acting as an electron donor (steps i–iii, Fig. 2) to the excited pyrenyl subunit acting as an electron acceptor.[11] It was found that among a number of metal ions tested (Fig. 1), Cr^{3+} enhanced both the intensity as well as quantum yield (Φ = 0.528) (33 fold) of the emission band owing to the formation of 1-aminopyrene (step iv, Fig. 2), compared to the free dyad **1**. As 1-ferrocenecarboxaldehyde and 1-aminopyrene have indeed been isolated (see ESI†) experimentally, it is proposed that the

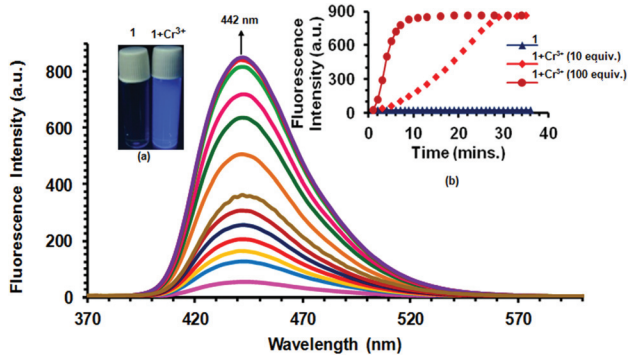

Fig. 3 Changes in the emission spectra of **1** (5.0×10^{-6} M, in THF) recorded after 5 min of addition of solution of Cr^{3+} (2.85×10^{-6} M to 5.0×10^{-4} M, in H_2O) (overall THF–H_2O ratio, 1 : 99 v/v). Inset: (a) visual change in fluorescence of **1** upon addition of 5.0×10^{-4} M Cr^{3+}, (b) revival of fluorescence of **1** in the presence of 10 and 100 equiv. of Cr^{3+}.

Cr^{3+} mediated hydrolysis of **1** leads to the formation of 1-aminopyrene due to which the fluorescence is turned '*on*'. It is reasonable to assume that Cr^{3+} species which otherwise quench fluorescence would also be present in the solution; we found that, compared to the higher fluorescence intensity and the quantum yield (Φ = 0.580) of the free 1-aminopyrene, the quantum yield (Φ = 0.526) decreases and matches with the value obtained in the present process.

The fluorometric titrations were conducted by adding increased concentrations of Cr^{3+} ions (2.85×10^{-6} M to 5.0×10^{-4} M, in H_2O) to a solution of **1** (5.0×10^{-6} M, in THF). A gradual increase in the intensity of the emission band centred at 442 nm was observed (Fig. 3). It is pertinent to mention that the increase in fluorescence continued until the addition of Cr^{3+} ions (5.0×10^{-5} M, in H_2O) with the detection limit of 1 μM (Fig. S5, see ESI†), but the process was completed only after 30 min of equilibration. However, when a higher concentration of Cr^{3+} (5.0×10^{-4} M, in H_2O) was employed, a similar increase in the fluorescence intensity could be achieved much faster (<10 min, Fig. 3 inset). The literature records detection of metal ions, where detection times ranging from 5 to 60 min

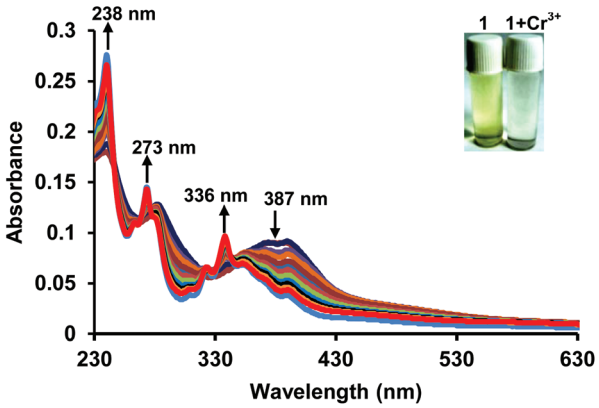

Fig. 4 Changes in the absorption spectra of **1** (5.0×10^{-6} M, in THF) upon addition of solution of Cr^{3+} (2.8×10^{-5} M to 5.0×10^{-4} M, in H_2O) (red). (The v/v ratio of THF and H_2O in the mixture was 1 : 99.) Inset: (a) visual change in color of **1** upon addition of 5.0×10^{-4} M Cr^{3+}.

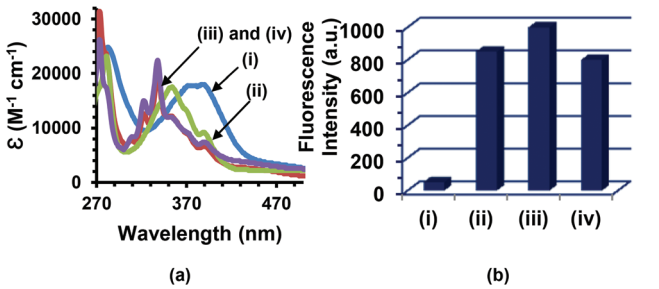

Fig. 5 (a) Absorption spectra and (b) emission profile (at 442 nm) of (i) **1**, (ii) 1-aminopyrene, (iii) **1** in the presence of 100 equiv. of Cr^{3+}, and (iv) 1-aminopyrene in the presence of Cr^{3+}, superimposed by (iii) in (a).

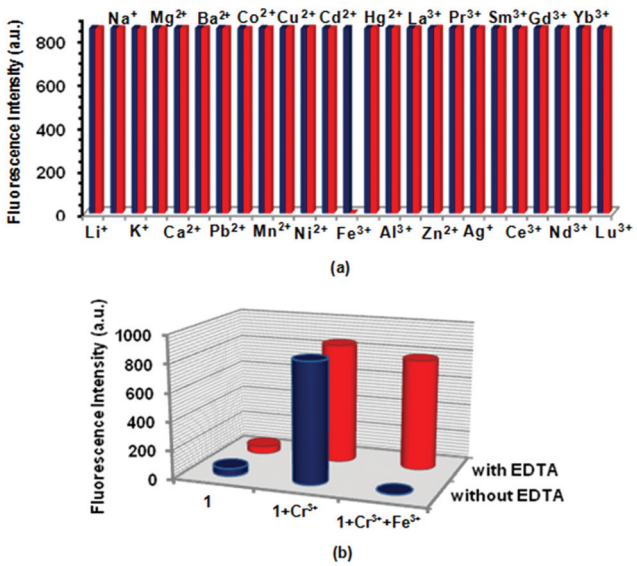

Fig. 6 (a) Emission of **1** (5.0×10^{-6} M, blue) in the presence of Cr^{3+} (5.0×10^{-4} M) and emission of **1** upon addition of Cr^{3+} (5.0×10^{-4} M, red) in the presence of other cations (5.0×10^{-4} M) in THF–H_2O (1 : 99 v/v); (b) emission properties of **1**, **1** + Cr^{3+} and **1** + Cr^{3+} + Fe^{3+} in the presence (red) and in the absence (blue) of 2.5 equiv. of EDTA, in THF–H_2O (1 : 99 v/v) (at 442 nm).

have been reported upon addition of 10–50 equiv. of the metal ions.[8b,c]

The UV-vis absorption spectrum of **1** (5.0×10^{-6} M, in THF) is characterized by a broad split band centred at 387 nm ($17\,800$ M^{-1} cm^{-1}) and two high energy bands at 283 and 238 nm ($14\,800$ and $22\,600$ M^{-1} cm^{-1} respectively) (Fig. 4). A low intensity broad band at 474 nm (4000 M^{-1} cm^{-1}) was also observed, which has a major contribution from the ferrocene based H−2 → L + 3 transition as deduced from the Gaussian 09 suite of programs.[12]

As the participating orbitals are located on the Fe atom and the cyclopentadienyl (Cp) moieties of ferrocene, it is assigned as a Fe^{2+}→Cp transition. Further, the split band at 387 nm has the main contribution from the HOMO (H) → LUMO (L) transition, with relatively little contribution from the H → L + 1 transition. The HOMO is mainly located on the pyrene, while the LUMO and the associated L + 1 are also mainly located on pyrene as well as the imine π-bridge; the transition (H → L + 1) corresponds mainly to the pyrene chromophore. The high energy transitions (273 and 238 nm) were assigned as intra-ligand transitions of **1**, based on the contributing orbitals (Fig. S6 and Tables S1 and S2, see ESI†).

Upon addition of an aqueous solution (5.0×10^{-4} M, in H_2O) of Cr^{3+} ions to a solution of **1** (5.0×10^{-6} M, in THF), while the band at 474 nm showed insignificant changes (Fig. 4) in intensity, the split bands centred at 387 nm showed both a decrease in intensity as well as blue shift. All these absorption changes were accompanied by appearance of a new band at 336 nm, the position as well as shape of which matched with the absorption spectrum of 1-aminopyrene in the presence of Cr^{3+} (Fig. 5a), recorded independently. A similar correlation could be observed in the emission profile also (Fig. 5b). Thus, the observed absorption and emission changes established the formation of 1-aminopyrene, giving support to the proposed hydrolysis of **1** (Scheme 1) in the sensing event.

The hydrolytic cleavage of **1** into its constituting precursors was further confirmed by recording the ^1H NMR spectrum of **1** in the presence of Cr^{3+} (1.0 equiv.) after equilibration, whereupon the signals corresponding to the hydrolytic products were clearly visualized (Fig. S7, see ESI†).

Based on the literature precedence,[8b] it is reasonable to assume that binding of the metal ion to the imine functionality may trigger its hydrolysis, to release 1-aminopyrene and 1-ferrocenecarboxaldehyde in solution, leading to chemodosimeter action of **1**. Further, the spectroscopic changes (fluorescence as well as absorbance) were not reversed upon addition of EDTA solution (Fig. 6), which is also expected for chemodosimeters. To rule out the possibility of an alternate mode of sensing through the formation of **1** : Cr^{3+} complex, when an independent reaction of **1** with $Cr(ClO_4)_3 \cdot 6H_2O$ was performed, we could only observe the formation of 1-ferrocenecarboxaldehyde and 1-aminopyrene (TLC, ^1H NMR, (Fig. S8) mass spectra (Fig. S9), see ESI†) and no Cr^{3+} complex could be isolated.

To check any interference from competitive metal ions, when the titration of Cr^{3+} was repeated in the presence of a number of metal ions (*vide experimental*), no interference was observed (Fig. 6a), except Fe^{3+} which quenched the emission intensity like many transition metals.[13] This might in fact limit the applicability of **1** to sense Cr^{3+} in those situations where Fe^{3+} is a contaminant and needs to be removed through precipitation (Fig. 6b) or other methods.[14]

Further, the effect of pH variation on **1** was also noted by recording the fluorescence spectra (Fig. S10, see ESI†)). Only a minor change was observed in the emission band of **1** in the pH range of 5–12, suggesting that **1** could be used in a physiological environment where the pH is >5 without resorting to the buffered media. However, an increase in the emission intensity with decreasing pH may also be attributed to the hydrolysis of the imine functionality as the Schiff-bases are known to undergo acid promoted hydrolysis.[15]

2.3. Application in cell imaging

In line with the reports[16] relating the role of heavy metal ions (including Cr^{3+}) to cell malignancy in breast cancer cells MCF-7, we employed **1** as an imaging agent for the detection of Cr^{3+} in MCF-7 cells. Interestingly, no cytotoxic effect was revealed even at higher dose (80 μM) used in the MTT assay[17] (Fig. 7), indicating that **1** could be employed as a highly viable chemosensor in biomedical research aimed at exploring the bioactivity of Cr^{3+} in biological systems.

Fig. 8 shows the confocal microscope images of MCF-7 cells treated with different concentrations of Cr^{3+}. The fluorescence was particularly visible in the perinuclear region of the cells as suggested by the overlay (Fig. 8a3–8g3) of fluorescence and bright field images indicating the subcellular distribution and excellent membrane permeability of **1**.

3. Conclusions

In conclusion, we have disclosed the '*turn-on*' fluorescent-based selectivity of a new pyrene–imine–ferrocene based dyad **1** for Cr^{3+}. The dyad **1** constitutes a simple and inexpensive chemodosimeter which demonstrates a highly viable and useful application for the detection of Cr^{3+} in solution as well as in biological samples.

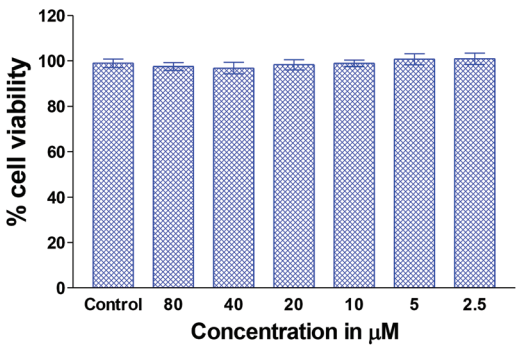

Fig. 7 MTT assay of breast cancer MCF7 cells cultured for 24 hours in media containing various concentrations of **1**.

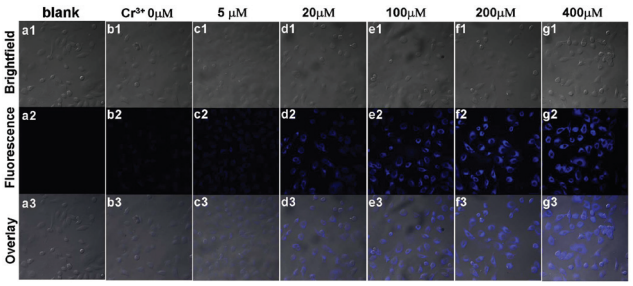

Fig. 8 Confocal images of MCF-7 cells, supplemented with varying concentration of $Cr(ClO_4)_3$ and **1** (5.0×10^{-6} M) (λ_{ex} 405 nm). a1–a3 were reference cells without **1**.

4. Experimental

4.1. Materials and general methods

Metal salts used in the spectrophotometric studies were of analytical grade and bought from Sigma-Aldrich. The solvents used were of analytical grade and purchased from Thomas Baker. Tetrahydrofuran (THF) was dried over sodium and benzophenone as an indicator. UV-vis and fluorescence studies were performed in dry THF and double distilled water. Biological cell imaging was done in 0.1 M PBS solution (pH = 7.2). Stock solutions (0.1 M) of perchlorate salts of Li^+, Na^+, Mg^{2+}, Ca^{2+}, Pb^{2+}, Ba^{2+}, Mn^{2+}, Co^{2+}, Ni^{2+}, Cu^{2+}, Hg^{2+}, Cr^{3+}, Fe^{3+} and nitrate salts of K^+, Ag^+, Zn^{2+}, Cd^{2+}, Al^{3+}, La^{3+}, Ce^{3+}, Pr^{3+}, Sm^{3+}, Gd^{3+}, Yb^{3+}, Nd^{3+}, Eu^{3+}, Tb^{3+}, Lu^{3+} ions were prepared in doubly distilled water. Stock solutions of dyad **1** (1×10^{-3} M) were prepared in THF. Test solutions (5.0×10^{-6} M) were prepared by taking 17.5 μM of the stock solution of dyad **1** and diluting the solution to 3.5 mL with water, and adding an appropriate aliquot of each metal stock (17.5 μM of 0.1 M stock solution to prepare 5.0×10^{-4} M).

IR spectra were recorded on a Perkin Elmer Spectrum Two-IR Fourier-Transform spectrophotometer in the range 400–4000 cm^{-1} using KBr as the medium. ^1H NMR (300 MHz) and ^{13}C NMR (75 MHz) spectra were recorded in $CDCl_3$ on a JEOL-FT NMR-AL spectrophotometer. Tetramethylsilane ($SiMe_4$) served as the internal standard and $CDCl_3$ (7.26 ppm for ^1H and 77.0 ppm for ^{13}C) was used as a solvent. Data are reported as follows: chemical shift in ppm (δ), multiplicity (s = singlet, m = multiplet), integration and interpretation. Mass spectra were recorded on a Bruker LC-MS microTOF II spectrometer. The purity of the products was checked by elemental analysis performed on a Thermoelectron FLASH EA1112 CHNS analyzer and were within ±0.4% of the theoretical values. Melting points were determined in open capillaries and are uncorrected. The fluorescence spectra were recorded on a Perkin Elmer LS 55 spectrofluorimeter with an excitation slit

width of 15.0 and an emission slit width of 2.5. UV-vis spectra were recorded on a SHIMADZU 1601 PC spectrophotometer with a quartz cuvette (path length, 1 cm) and studies were performed in AR grade THF and double distilled water. The cell holder of the spectrophotometer was maintained at 25 °C for consistency in the recordings. The biological cell imaging was carried out on the NIKON A1R confocal microscope.

4.2. Synthesis of (1*E*)-*N*-(ferrocenylmethylene)pyren-1-amine (1)

To a solution of 1-pyreneamine (217 mg, 1.0 mmol) in ethanol (15 mL) was added 2 drops of formic acid. To this was added a solution of 1-ferrocenecarboxaldehyde[18] (214 mg, 1.0 mmol) in ethanol (15 mL) under a nitrogen atmosphere. The reaction mixture was stirred at room temperature for one hour. The resulting solid was filtered and recrystallized in an ethanol–chloroform (3 : 1) mixture to afford **1** as a dark red solid (384 mg, 74%); mp: >200 °C. IR (KBr): ν_{max}/cm^{-1} 3040 (aromatic C–H), 1615 (pyrene C=C), 1590 (C=N), 1104 (Cp). ^{1}H NMR (300 MHz, $CDCl_3$, 25 °C): δ 4.34 (s, 5H, Cp*H*), 4.58 (s, 2H, Cp*H*), 4.99 (s, 2H, Cp*H*), 7.64 (s, 1H, N=C*H*), 7.96–8.17 (m, 7H, aromatic C*H*), 8.57 (s, 2H, aromatic C*H*) ppm. ^{13}C NMR (75 MHz, $CDCl_3$, 25 °C): 69.212, 69.393, 71.478, 80.865, 122.823, 122.955, 123.227, 124.208, 124.694, 124.909, 125.576, 126.054, 126.236, 126.895, 127.365, 127.909, 131.568, 131.873, 134.576, 162.309 ppm. MS (EI): *m*/*z* 414.09 (M^+ + 1). Anal. calcd (%) for $C_{27}H_{19}NFe$ (413.09): C, 78.45; H, 4.60; N, 3.39. Found: C, 78.32, H, 4.51, N, 3.33 (Fig. S1–S4, see ESI†).

4.3. Quantum yield calculations

The fluorescence quantum yields were determined using an optically matching solution of 9,10-diphenylanthracene as a standard having a quantum yield of 0.86 in cyclohexane[19] using the equation:

$$\Phi_x = \Phi_{st} \times (F_x A_{st} \times \eta_x{}^2)/(F_{st} A_x \times \eta_{st}{}^2)$$

where Φ_x and Φ_{st} are the quantum yields of the test sample and the standard sample respectively, A_x and A_{st} are the absorbances of the test sample and the standard sample respectively, F_x and F_{st} are the areas of emission bands for the test sample and the reference sample, η_x and η_{st} are the refractive indices of test sample and standard sample solutions in their respective pure solvents.

4.4. Computational methods

All theoretical calculations were carried out using the Gaussian 09 suite of programs. The molecular geometries of the chromophores were optimized at the density functional theory (DFT) calculations employing the hybrid B3LYP[20] functional. The 6-31G* basis set was used for C and H, aug-cc-pVTZ for the donor N atom and LANL2DZ with effective core potential for the metal atom Fe. The frequency calculations were also performed using the same method and basis sets. The frequency analysis indicates that the optimized geometry is the true energy minimum because no imaginary frequency is found. Energy values and properties of the systems were computed considering solvent (water) effects by using Cossi and Barone's CPCM (conductor-like polarizable continuum model) modification[21] of Tomasi's PCM formalism.[22] The first 30 excited states were calculated by using time-dependent density functional theory (TD-DFT calculations). The molecular orbital contours were plotted using Gauss view 5.0.9.

4.5. Cytotoxicity assay

To check that the cytotoxic effect of **1**, MCF-7 cells were seeded at 3×10^3 cells per well in 100 μl DMEM containing 10% FBS in a 96-well tissue culture plate and incubated for 48 h at 37 °C (till 50% confluence), 5% CO_2 in air and 90% relative humidity in CO_2 incubator. After incubation, 100 μl of **1** solution (80, 40, 20, 10 and 5 μM), prepared in DMEM, was added to cells and the cultures were incubated for 24 hours. Four hours before the termination of the experiment, the medium was discarded and 100 μl DMEM containing MTT [3-(4,5-dimethylthiazol-2-yl)-2,5-diphenyltetrazolium bromide] (5 mg ml^{-1}) was added to the cells and incubated in a CO_2 incubator at 37 °C in the dark for 4 hours. After incubation, the purple colored formazan produced in the cells appeared as dark crystals at the bottom of the wells. The culture medium was aspirated from each well carefully to prevent disruption of the cell monolayer. At last, 100 μl of DMSO was added into all wells and mixed thoroughly to dissolve the formazan crystals, producing a purple solution. The absorbance of the 96 well plates was taken at 570 nm with a Labsystems Multiskan EX ELISA reader against a reagent blank. The cytotoxic effect of each treatment was expressed as percentage of cell viability relative to the untreated control cells.

4.6. Live cell imaging studies

Human breast adenocarcinoma MCF-7 cell line was obtained from NCCS, Pune, India and maintained on Dulbecco's modified Eagle's medium (DMEM) supplemented with streptomycin (100 U ml^{-1}), gentamycin (100 μg ml^{-1}), and 10% FBS (Sigma-Aldrich) at 37 °C and a humid environment containing 5% CO_2. For imaging, MCF-7 cells were cultured on 18 mm glass coverslips in 12 well plates at 2×10^4 cells per well and allowed to grow for 48 hours (till 70–80% confluence). Experiments to assess Cr^{3+} uptake were performed in the same media supplemented with different concentrations of $Cr(ClO_4)_3 \cdot 6H_2O$ (5, 20, 100, 200, 400 μM) for 2 hours. Cells were washed twice with phosphate buffered saline before incubating with 5 μM of **1** in PBS for 20 min at 25 °C. The cells were again washed twice with PBS before imaging. Confocal imaging of MCF-7 cells was achieved using a NIKON AIR confocal laser scanning microscope using a diode laser with excitation at 405 nm. Imaging was carried out with Plan Apo 40× objective lens.

Acknowledgements

PK thanks UGC 41-232/2012(SR), New Delhi for the financial help and KS thanks UGC SAP DRS-I. MK acknowledges UGC for the research fellowship.

Notes and references

1 (*a*) A. K. Singh, V. K. Gupta and B. Gupta, *Anal. Chim. Acta*, 2007, **585**, 171–178; (*b*) J. B. Vincent, *Nutr. Rev.*, 2000, **58**, 67–72.
2 S. Latva, J. Jokiniemi, S. Peraniemi and M. Ahlgren, *J. Anal. At. Spectrom.*, 2003, **18**, 84–86.
3 A. M. Zayed and N. Terry, *Plant Soil*, 2003, **249**, 139–156.
4 Y. Li, C. Chen, B. Li, J. Sun, J. Wang, Y. Gao, Y. Zhao and Z. Chai, *J. Anal. At. Spectrom.*, 2006, **21**, 94–96.
5 A. W. Varnes, R. B. Dodson and E. L. Wehry, *J. Am. Chem. Soc.*, 1972, **94**, 946–950.
6 (*a*) P. Mahato, S. Saha, E. Suresh, R. Di Liddo, P. P. Parnigotto, M. T. Conconi, M. K. Kesharwani, B. Ganguly and A. Das, *Inorg. Chem.*, 2012, **51**, 1769–1777; (*b*) S. Saha, P. Mahato, G. U. Rreddy, E. Suresh, A. Chakrabarty, M. Baidya, S. K. Ghosh and A. Das, *Inorg. Chem.*, 2012, **51**, 336–345; (*c*) Y. Wan, Q. Guo, X. Wang and A. Xia, *Anal. Chim. Acta*, 2010, **665**, 215–220; (*d*) K. Huang, H. Yang, Z. Zhou, M. Yu, F. Li, X. Gao, T. Yi and C. Huang, *Org. Lett.*, 2008, **10**, 2557–2560; (*e*) Z. Zhou, M. Yu, H. Yang, K. Huang, F. Li, T. Yi and C. Huang, *Chem. Commun.*, 2008, 3387–3389.
7 (*a*) P. Kaur, D. Sareen and K. Singh, *Dalton Trans.*, 2012, **41**, 9607; (*b*) P. Kaur, D. Sareen and K. Singh, *Dalton Trans.*, 2012, **41**, 8767; (*c*) P. Kaur, M. Kaur and K. Singh, *Talanta*, 2011, **85**, 1050–1055.
8 (*a*) M. H. Lee, T. V. Giap, S. H. Kim, Y. H. Lee, C. Kang and J. S. Kim, *Chem. Commun.*, 2010, 1407–1409; (*b*) J. H. Kim, H. J. Kim, C. W. Bae, J. W. Park, J. H. Lee and J. S. Kim, *ARKIVOC*, 2010, 170–178; (*c*) W. Lin, L. Yuan, J. Feng and X. Cao, *Eur. J. Org. Chem.*, 2008, 2689–2692.
9 F. M. Winnick, *Chem. Rev.*, 1993, **93**, 587–614.
10 (*a*) F. Oton, M. del C. Gonzalez, A. Espinosa, A. Tarraga and P. Molina, *Organometallics*, 2012, **31**, 2085–2096; (*b*) D. Zhang, Q. Zhang, J. Su and H. Tian, *Chem. Commun.*, 2009, 1700–1702; (*c*) T. Romero, A. Caballero, A. Tarraga and P. Molina, *Org. Lett.*, 2009, **11**, 3466–3469; (*d*) R. Martinez, A. I. Ratera, A. Tarraga, P. Molina and J. Veciana, *Chem. Commun.*, 2006, 3809–3811.
11 D. Albagli, G. C. Bazan, R. R. Schrock and M. S. Wrighton, *J. Phys. Chem.*, 1993, **97**, 10211–10216.
12 M. J. Frisch, *et al.*, *Gaussian 09 (REVISION B.01)*, Gaussian, Inc., Wallingford, CT, 2010, for the complete reference see ESI.†
13 (*a*) S. S. Tan, S. J. Kim and E. T. Kool, *J. Am. Chem. Soc.*, 2011, **133**, 2664–2671; (*b*) A. M. Funston, K. P. Ghiggino, M. J. Grannas, W. D. McFadyen and P. A. Tregloan, *Dalton Trans.*, 2003, 3704–3712.
14 M. A. Al-Anber, *Desalination*, 2010, **250**, 885–891.
15 (*a*) T. Okuyama, H. Nagamatsu, M. Kitano and T. Fueno, *J. Org. Chem.*, 1986, **51**, 1516–1521; (*b*) C. Suksai and T. Tuntulani, *Chem. Soc. Rev.*, 2003, **32**, 192–202.
16 S. Yaghoubi, J. Barlow and P. H. Kass, *Breast Cancer and Metals: A Literature Review*, Zero Breast Cancer Non-Profit Organization, 2007.
17 L. V. Rubinstein, K. D. Paul, R. M. Simon, P. Skehan, D. A. Scudiero, A. Monks and M. R. Boyd, *J. Natl. Cancer Inst.*, 1990, **82**, 1113–1117.
18 M. Rosenblum, A. K. Banerjee, N. Danieli, R. W. Fish and V. Schlatter, *J. Am. Chem. Soc.*, 1963, **85**, 316–324.
19 J. V. Morris, M. A. Mahaney and J. R. Huber, *J. Phys. Chem.*, 1976, **80**, 969–974.
20 L. J. Bartolotti and K. Flurchick, in *Reviews in Computational Chemistry*, ed. K. B. Lipkowitz, B. D. Boyd, VCH, New York, 1996, vol. 7, pp. 187–216.
21 (*a*) M. Cossi, N. Rega, G. Scalmani and V. Barone, *J. Comput. Chem.*, 2003, **24**, 669–681; (*b*) V. Barone and M. Cossi, *J. Phys. Chem. A*, 1998, **102**, 1995–2001.
22 (*a*) R. Cammi, B. Mennucci and J. Tomasi, *J. Phys. Chem. A*, 2000, **104**, 5631–5637; (*b*) S. Miertus, E. Scrocco and J. Tomasi, *Chem. Phys.*, 1981, **55**, 117–129.

